Naval Research Laboratory

Washington, DC 20375-5320

NRL/MR/6120--01-8585

A Review of the Crystal Structures of Common Explosives Part I: RDX, HMX, TNT, PETN, and Tetryl

G. R. MILLER

University of Maryland
College Park, MD

A. N. GARROWAY

Materials Chemistry Branch
Chemistry Division

October 15, 2001

REPORT DOCUMENTATION PAGE

Form Approved
OMB No. 0704-0188

1. AGENCY USE ONLY (*Leave Blank*)	2. REPORT DATE	3. REPORT TYPE AND DATES COVERED
	October 15, 2001	Subject matter report (Part II)

4. TITLE AND SUBTITLE

A Review of the Crystal Structures of Common Explosives
Part I: RDX, HMX, TNT, PETN, and Tetryl

5. FUNDING NUMBERS

FAA DTFA0300X90011
Army MIPR1BP1C00114
ONR N0001401WX20564

G.R. Miller* and A.N. Garroway

7. PERFORMING ORGANIZATION NAME(S) AND ADDRESS(ES)

Naval Research Laboratory
4555 Overlook Avenue, SW
Washington, DC 20375-5320

8. PERFORMING ORGANIZATION REPORT NUMBER

NRL/MR/6120--01-8585

9. SPONSORING/MONITORING AGENCY NAME(S) AND ADDRESS(ES)

Director, Federal Aviation Administration William J. Hughes Technical Center (Attn: Dr. Ronald A. Krauss), AAR-520, Atlantic City Airport NJ 08405
Commanding Officer, USACECOM-NVESD (Attn: Ms Vivian George), PM-MCD, AMSTA-DSA-MC, 10205 Burbeck Road, Fort Belvoir, VA 22060-5811
Commanding Officer, Office of Naval Research (Attn: Mr. Thomas J. Singleton), Code 09A, BCT1, Room 1216, 800 North Quincy Street, Arlington, VA 22217-5660

10. SPONSORING/MONITORING AGENCY REPORT NUMBER

11. SUPPLEMENTARY NOTES

*U. MD ASEE/NRL summer faculty

12a. DISTRIBUTION/AVAILABILITY STATEMENT

Approved for public release; distribution is unlimited.

12b. DISTRIBUTION CODE

13. ABSTRACT (*Maximum 200 words*)

The purpose of this review is to provide those who are working on explosive detection techniques with descriptions of the various crystalline forms of these common explosives, the conditions under which phase transitions between these forms are observed, the molecular structures found in the various crystalline phases, and a critical evaluation of the X-ray and neutron diffraction studies that determined these structures. Here we consider the crystal and molecular structures of RDX, HMX, TNT, PETN, and Tetryl; Part II of our review will cover ammonium nitrate, NH_4NO_3.

14. SUBJECT TERMS

Explosives	Aviation security	Diffraction
Explosives detection	X-ray	Neutron diffraction
Landmines	Crystal structure	Polymorphism

15. NUMBER OF PAGES

33

16. PRICE CODE

17. SECURITY CLASSIFICATION OF REPORT	18. SECURITY CLASSIFICATION OF THIS PAGE	19. SECURITY CLASSIFICATION OF ABSTRACT	20. LIMITATION OF ABSTRACT
UNCLASSIFIED	UNCLASSIFIED	UNCLASSIFIED	UL

NSN 7540-01-280-5500

Standard Form 298 (Rev. 2-89)
Prescribed by ANSI Std 239-18
298-102

Table of Contents

A Review of the Crystal Structures of Common Explosives Part I: RDX, HMX, TNT, PETN, and Tetryl

Overview

The purpose of this review is to provide those who are working on explosive detection techniques with descriptions of the various crystalline forms of these common explosives, the conditions under which phase transitions between these forms are observed, the molecular structures found in the various crystalline phases, and a critical evaluation of the X-ray and neutron diffraction studies that determined these structures. Here we consider the crystal and molecular structures of RDX, HMX, TNT, PETN, and Tetryl; Part II of our review will cover ammonium nitrate, NH_4NO_3.

Mino Caira has recently written a very useful review on crystal polymorphism,[1] treating the thermodynamic, kinetic, and structural aspects of polymorphism and discussing many practical problems and modern techniques for studying polymorphism. That review begins with references to other reviews published in the previous decade. Walter McCrone, who did much of the early work on the morphology of the crystal forms of various explosives, wrote an introduction to polymorphism[2] in 1965 that's still useful today. He included treatments of the thermodynamics and the kinetics of these phase changes, some of which are illustrated with examples drawn from work on HMX, RDX, and TNT (though the work on TNT in particular is incomplete and outdated.) A short review of some useful elements of crystallography and some references to more complete treatments of crystallography are contained in the Appendix.

There has been significant progress recently on theoretical efforts to predict the crystal structures and the relative stabilities of polymorphs for a wide variety of explosives.[3, 4, 5, 6, 7, 8] These predictions are based on molecular packing and molecular dynamics calculations employing known atomic radii and calculated partial charges within the molecules. In some cases, the effects of both temperature and pressure are modeled.

RDX: (CAS Name and Registry Number: hexahydro-1,3,5-trinitro-1,3,5-triazine, *[121-82-4]*; other names: 1,3,5-trinitro-1,3,5-triazacyclohexane; 1,3,5-trinitrohexahydro-1,3,5-triazine; cyclo-trimethylenetrinitramine; Hexogen; Cyclonite). $C_3H_6N_6O_6$.

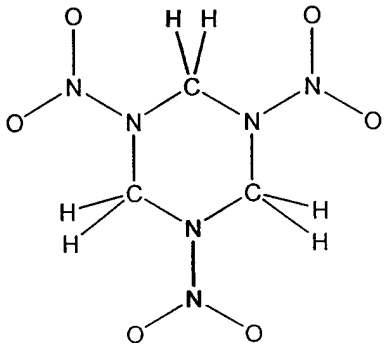

FIGURE 1. RDX

Manuscript approved September 17, 2001.

RDX consists of alternating CH_2 and N-NO_2 groups in a puckered, six-membered ring (Fig. 1). It melts with decomposition at 205°C and readily sublimes below the melting point. The definitive crystal structure of the stable form of RDX at room temperature, α-RDX, is the neutron diffraction study of Choi and Prince,[9] which is based on the X-ray structure determination of Harris and Reed.[10] (Earlier x-ray studies were done by Terpstra[11] and Hultgren.[12]) The crystal structure is orthorhombic. In Table 1, the Hermann-Mauguin notation for the space group is given first, with the Schoenflies notation given in parentheses; the unit cell lengths are given next; the number of formula units (in this case, the number of molecules) in the unit cell, *Z* is given next; finally, the measured density and the density calculated from the unit cell parameters and the molecular weight are shown.

TABLE 1
The Crystal Structure of α-RDX

Space Group	*a*	*b*	*c*	*Z*	Density (meas.)	Density (calc.)
Pbca (V_h^{15})	13.182 (2)	11.574 (2)	10.709 (2) Å	8	1.816	1.806 g/cc

The molecule is distorted in the solid from the expected three-fold symmetry (Fig.2), with one NO_2-group nearly co-planar with the adjacent NC_2-group. The two nitrogen atoms of this nitramine group (N(1) and N(4)) lie in a pseudo-mirror plane bisecting the molecule. The other two NO_2-groups are in nearly equivalent positions pointing down away from the six-membered ring.

Diamond anvil cell studies of RDX by Russell *et al*[13], show that both a γ-form and a β-form exist at sufficiently high pressures. γ-RDX (also orthorhombic) is stable above 3.8 GPa (38,000 atm.) between room temperature and 225°C, but spontaneously reverts to α-RDX when the pressure is reduced to 3.5 GPa. β-RDX is stable above 225°C from 2.5 - 7 GPa; it reverts to the α-form when the pressure is reduced to close to 1 atm.

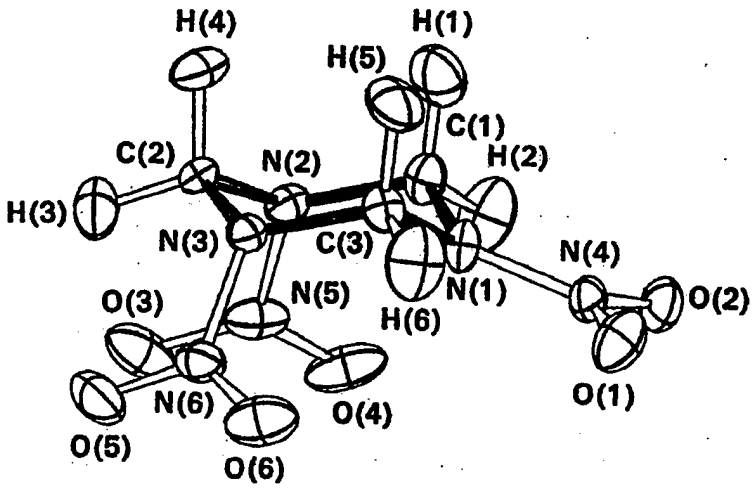

FIGURE 2. The structure of the RDX molecule in α-RDX (from Choi and Prince[9])

Sorescu, Rice, and Thompson[3] developed an intermolecular potential for calculating the crystal structure of RDX - later applied to many other explosives - and were successful in obtaining the known structure as the most stable structure. These calculations also yielded thermal expansion coefficients in reasonable agreement with experiment. In later work,[8] they extended these calculations on RDX to show the effect of hydrostatic compression on the lattice parameters (which agrees with experiment).

McCrone[14] has optically detected an unstable polymorph prepared by recrystallizing RDX on a microscope slide from a high boiling solvent such as nitrobenzene or TNT. This form transforms into α-RDX within seconds of preparation. McCrone also has the most complete description of the crystal morphology of α-RDX.

Cady[15] reports that RDX (as well as TNT and PETN) forms large single crystals from ethyl acetate solutions; these crystals have conical rather than flat faces where the cone angles are typically several tenths of a degree less than 180°. He speculates that the crystal defects giving rise to these conical faces and to ideally mosaic crystals may be responsible for twinning and the polymorphism of some explosives. (Fuller discussion of Cady's evidence and speculations are in the PETN section, below.)

While several unsymmetrical cyclic nitramines are known to form plastic crystalline phases below their melting point, RDX does not.[16]

Several of the methods used to produce RDX also produce measurable amounts of HMX as well.[17] Both of these explosives may contain small amounts of the other, either as entrained crystals or in solid solution.

HMX: (CAS Name and Registry Number: octahydro-1,3,5,7-tetranitro-1,3,5,7-tetrazocine, *[2691-41-0]*; other names: 1,3,5,7-tetranitro-1,3,5,7-tetrazacyclo-octane; cyclotetramethylenetetranitramine; Octogen; Homocyclonite). $C_4H_8N_8O_8$.

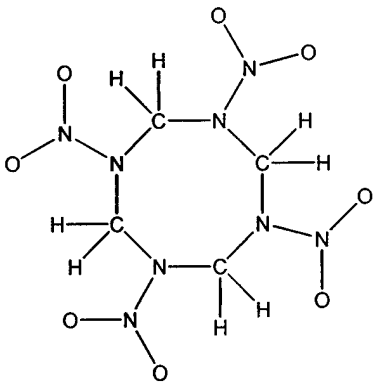

FIGURE 3. HMX

HMX consists of alternating CH_2 and N-NO_2 groups in an eight-membered, puckered ring (Fig. 3). It has a melting point of 282°C. The ring is fairly flexible and it can assume a variety of conformations.

McCrone[18] has described the crystal morphologies of the four different crystalline forms known for HMX, and two naming systems are present in the explosives literature (Table 2). There is considerable disagreement in the early literature on the transition temperatures.[18, 19, 20] Even the $\beta \rightarrow \alpha$ transition is reported to occur from as low as 102 °C to as high as 150 °C. The disagreements continue in the later literature (cf. Figure 7 and Table 7 in this review). McCrone[18] and Cady and Smith[19] give the crystallization conditions for preparing the various modifications.

TABLE 2
Crystal Structures of HMX

Name	Alternate Name	Crystal System	Density (meas.)	Stability Range[21]
β-HMX	HMX I	Monoclinic	1.90 g/cc	Room temperature to 115°C
α-HMX	HMX II	Orthorhombic	1.84	115 - 156°C
γ-HMX*	HMX III	Monoclinic	1.76	~156°C
δ-HMX	HMX IV	Hexagonal	1.80	156 - m.p. (280 - 281.5°C)

*Now known to be a hydrate and not a true polymorph of HMX.

Explosive sensitivity: It is generally agreed that the sensitivities are $\delta > \gamma > \alpha > \beta$, but Cady and Smith[19] found wide, unexplained variability in the sensitivity of the α form and a dependence on particle size (larger particles are more sensitive) for the γ form.

β-HMX: The definitive crystal structure of the thermodynamically stable form of HMX at room temperature, β-HMX, is the neutron-diffraction study of Choi and Boutin[22], based on the refinement of the crystal structure by Cady, Larson, and Cromer[23] of the x-ray structure determined by Eiland and Pepinsky.[24] The crystal structure (Table 3) is monoclinic (cf. Appendix for a description of the various conventions for describing the one non-90° interaxial angle).

TABLE 3
Crystal Structure of β-HMX

Space Group	*a*	*b*	*c*	β	Z	Density (meas.)	Density (calc.)
$P2_1/c$ (C_{2h}^5)	6.54	11.05	8.70 Å	124.3°	2	1.90	1.894

This is the most dense and least impact-sensitive polymorph of HMX. The HMX molecule is found to be centrosymmetric in β-HMX (Fig.4), so this conformer has a zero electric dipole moment. Two structurally different, adjacent nitramine groups are "up" and the symmetrically related pair of nitramine groups are "down" on the puckered ring. Within each of the structurally different nitramine groups, there is a short H···O contact (2.19 Å for one nitramine group, 2.34 Å for the other) which results in the carbon atom of the C–H···O intra-molecular hydrogen bond being pulled out of the plane of the rest of the nitramine group (0.459 Å and 0.224 Å, respectively). The eight-membered ring has a short, 2.77 Å distance between one pair of symmetrically located ring nitrogens and an elongated, 3.77 Å distance between the other pair of symmetrically located ring nitrogens. All of the

hydrogen atoms are involved in short, intermolecular H···O contacts, some as short as 2.36 Å.

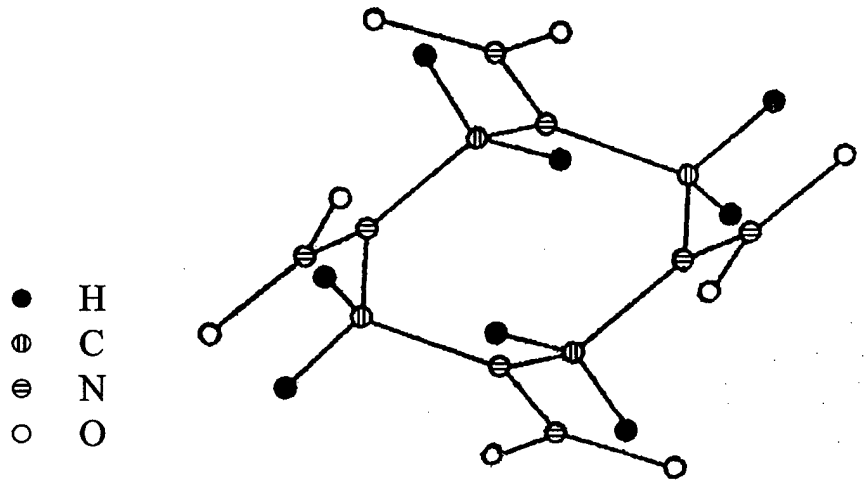

FIGURE 4. The structure of the HMX molecule in β-HMX (from Choi and Boutin[22])

Armstrong *et al*[25] have done calculations on the energetics of twinning in β-HMX (based on Howard Cady's privately communicated observations (published simultaneously[15]) of growth twinning and of deformation twinning on the 101 plane of the monoclinic structure. Although they report that HMX is twice as hard as RDX as measured by the Vickers diamond pyramid hardness (VHN) test, the mechanism for twinning in β-HMX depends on flexing of intramolecular bonds within the HMX molecule - a more flexible molecule than RDX. This twinning involves both a molecular rotation and a translation.

α-HMX: Cady *et al*[23] determined the crystal structure of α-HMX and have provided a comparison of the crystal structures of the four polymorphs of HMX. The crystal structure of α-HMX is orthorhombic (Table 4). The HMX molecule has a two-fold symmetry axis and all four NO_2 groups are on the same side of the ring (Fig.5), yielding a conformer with a large electric dipole moment.

TABLE 4
Crystal structure of α-HMX

Space Group	*a*	*b*	*c*	Z	Density (meas.)	Density (calc.)
*Fdd*2 (C_{2h}^{19})	15.13	23.89	5.913 Å	8	1.84	1.839

Choi and Boutin[22] provide a comparison of the bond lengths in α-HMX and β-HMX. For the bonds not involving H (which are poorly determined in the X-ray structure of α-HMX), the bond lengths are essentially the same in the two crystalline forms, often agreeing within 0.01 Å (the largest deviation is 0.034 Å).

Though not thermodynamically stable at room temperature, pure α-HMX can be prepared by

suitable choice of solvent and crystallization conditions[18,19] and kept indefinitely at room temperature in the absence of solvent. α-HMX forms at an evaporating solvent-container interface, whether or not β-HMX is present, conditions likely to be encountered in the processing of explosives.[19]

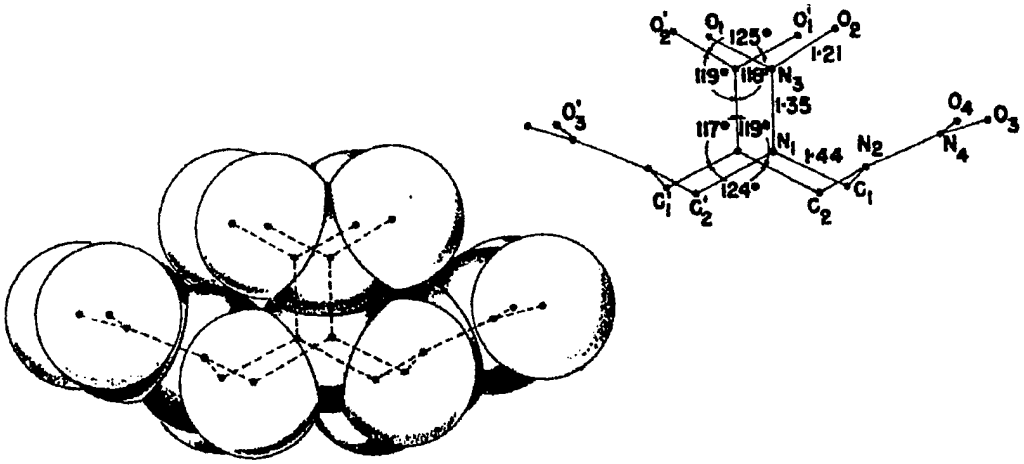

FIGURE 5. The structure of the HMX molecule in α-HMX (from Cady, Larson, & Cromer[23])

γ-HMX: The unit cell dimensions for γ-HMX (monoclinic) have been published by Cady *et al*[23] and the crystal structure has been determined by Main, Cobbledick, and Small[26] (Table 5).

TABLE 5
Crystal Structure of γ-HMX ($2\,C_4H_8N_8O_8 \cdot 0.5\,H_2O$)

Space Group	*a*	*b*	*c*	β	Z	Density (meas.)	Density (calc.)	Authors
Pc, *P2/c* (C_{2h}^4), or *P2/n*	10.95	7.93	14.61	119.4°	4	1.76	1.78	Cady, Larson, & Cromer[23]
(Alternate indexing)	13.28	7.93	10.95	106.5°	4			
Pn	13.27	7.90	10.95	106.8°	2	1.78	1.82	Main, Cobbledick & Small[26]

γ-HMX is not a true polymorph of HMX but rather a hydrate, $2\,C_4H_8N_8O_8 \cdot 0.5\,H_2O$. (The two HMX molecules in the formula of the hydrate account for the difference between Z = 4 and Z = 2 (formula units/unit cell) in the table above.) Main *et al*[26] postulate a 50% occupancy rate for the oxygen position of the water molecule in the structure, based on the electron density found at that position. Their Karl Fisher determination of water in their sample found 1.18(15)% water, somewhat less than the 1.47% by weight for the specified composition. They confirmed the presence of water by observing the O-H stretching frequencies in the IR spectrum of their γ-HMX. Hermann, Engel, and

Eisenriech,[27] on the other hand, could not detect the loss of water when the sample was heated in a thermobalance or in an IR cell, and their Karl Fischer analysis failed to detect the amount of water Main *et al* detected. Hermann *et al* did find evidence for the growth and disappearance of a shifted X-ray peak upon heating in the 120 - 180 °C range which they assume is due to the loss of water from the lattice of γ-HMX; no reverse effect was observed upon cooling the sample, consistent with the model of water loss upon heating.

There are two kinds of HMX molecules in the unit cell, but the shape, bond lengths, and bond angles are almost the same. Each HMX molecule has a conformation nearly that of the HMX molecule in α-HMX, but without the perfect two-fold symmetry found in the α form. The water molecule sits in a void with the oxygen atom located 2.9 - 3.1 Å away from four oxygen atoms in HMX molecules, distances consistent with quite weak hydrogen bonding (the hydrogen atoms of the water molecule were not located.)

γ-HMX can be prepared by suitable choice of solvent and crystallization conditions[18, 19] and some preparations can be kept indefinitely at room temperature in the absence of solvent. γ-HMX is formed during steam distillation of HMX solutions and on precipitation from water-miscible solvents by dilution with water, conditions found in the processing of explosives and in the preparation of plastic-bonded explosives by the water-slurry method.[19]

δ-HMX: The unit cell dimensions for δ-HMX (hexagonal) have been published by Cady *et al*[23] and the crystal structure has been determined by Cobbledick and Small[28] (Table 6).

TABLE 6
Crystal structure of δ-HMX

Space Group	*a*	c	Z	Density (meas.)	Density (calc.)	Authors
$P6_122$ (D_6^2) or $P6_522$ (D_6^3)	7.66	32.49	6	1.80	1.786	Cady, Larson, & Cromer[23]
$P6_1$ (C_6^2) or $P6_5$ (C_6^3)	7.711 (2)	32.553 (6)	6	1.58	1.586*	Cobbledick & Small[28]

* This calculated density must be in error and both the calculated and the measured densities reported in this paper are probably transcription errors. Given the unit cell dimensions determined in this paper and the molecular weight of HMX, the calculated density is 1.760, in reasonable agreement with Cady *et al.*

The HMX molecules in δ-HMX have a single conformation which is nearly the same as the molecules in α-HMX. The bond lengths and bond angles are nearly the same but the molecules do not have the perfect two-fold symmetry found in α-HMX.

δ-HMX can be prepared by suitable choice of solvent and crystallization conditions,[18, 19] but the solid-solid transformation to the β form can take place in the presence of β-HMX as described below.

Solid-solid polymorphic transformations: Cady and Smith[19] have a fairly extensive

discussion of their observations of transformations between the various crystal structures, which is summarized below.

- Pure samples of the unstable polymorphs rarely transform into β-HMX at room temperature except in the presence of solvent or solvent vapor (so the absence of solvent apparently leads to kinetic stability).
- The β → δ transition about 159 °C is the most commonly observed transition. β-HMX is commonly found to have several percent RDX present, some of which appears to be in solid solution in the HMX. Unless special efforts are made, purified forms of β-HMX appear to still have about 0.1% RDX in solid solution with no evidence for crystalline RDX. The presence of RDX was found to facilitate the conversion from β-HMX to δ-HMX, beginning at 159 °C. RDX-free β-HMX will not transform to the δ form below 170 °C. They attribute the effect of RDX to an apparent ease in forming slip plane imperfections under stress. If δ-HMX and β-HMX are in intimate contact, the solid-solid transformation to β-HMX will occur at room temperature. Pure δ-HMX can be stored indefinitely without transforming to the β form.
- The β → α transformation occurs when β-HMX is heated between 170 and 190 °C, with more α produced the lower the RDX content of the HMX. The reverse solid-solid transformation has not been observed.
- The β → γ transformation was not observed. The reverse transformation does occur in the solid phase at room temperature, particularly for γ crystals which have been strained, but the transformation is not as easy as the δ → β transformation.
- The α → δ transition occurs above 190 °C. The reverse solid-solid transformation has not been observed.

Using X-ray diffraction, Hermann *et al,*[27, 29] have measured the lattice constants of all four polymorphs as a function of temperature from 173 K (-100 °C) to the vicinity of 493 K (220 °C) and have plotted the volume per molecule *vs.* temperature (Fig.6).

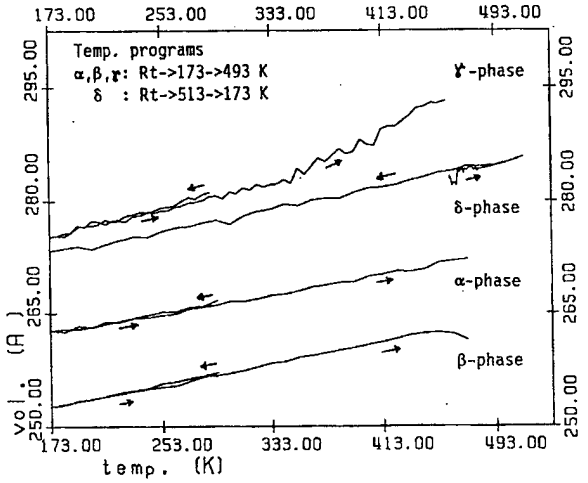

FIGURE 6. Volume (Å^3) per HMX molecule in α-, β-, γ-, and δ-HMX as a function of temperature (K) (from Hermann, Engel, and Eisenreich[27])

Upon heating, β-HMX shows an anomalous shrinking over the 20° range before the phase transition, a shrinking which is not reversed upon re-cooling the sample. γ-HMX shows an increased expansion coefficient above 350 K (77 °C). By measuring the intensities of certain reflections as a function of temperature, Hermann *et al*[27] were able to follow the β → δ, α → δ, and γ → δ phase transformations (Fig.7).

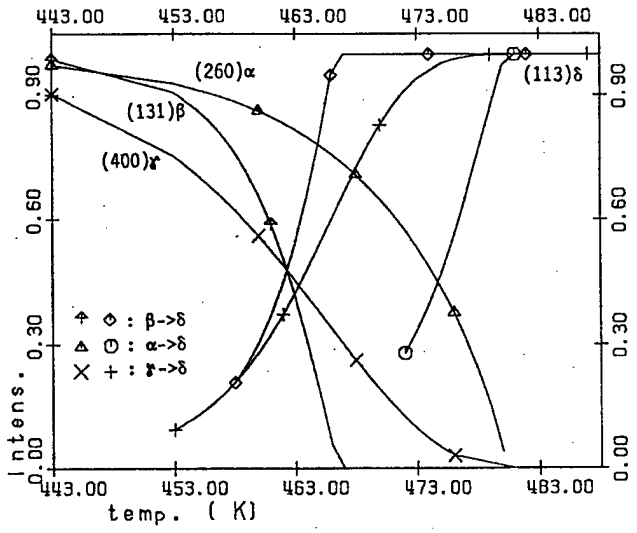

FIGURE 7. The intensities of the X-ray diffraction peaks 131 (β-HMX), 260 (α-HMX), 400 (γ-HMX), and 113 (δ-HMX) as a function of temperature (K), given as a percentage of the intensity of the diffraction peak in the pure polymorph (from Hermann, Engel, and Eisenreich[27])

The differential scanning calorimetry data of Hermann *et al*[27] show transition temperatures for the phase transitions (Table 7) similar to those found in the X-ray data in Figure 7, but both sets of transition temperatures are higher than those reported by Urbanski[21] (cf. the initial discussion of HMX transition temperatures and Table 2 in this review).

TABLE 7
HMX Phase transition temperatures (DSC).

β → δ	454 - 466 K (181 - 193°C)
α → δ	461 - 467 K (188 - 194°C)
γ → δ	444 - 455 K (171 - 182°C)

While a number of unsymmetrical cyclic nitramines are known to undergo a phase transition to a plastically crystalline phase at high temperature, HMX does not.[16]

Sorescu *et al*[5,6] have shown that the lattice energies of the three true polymorphs of HMX are in accord with the stabilities β > α > δ (Table 8). They also have calculated the thermal expansion coefficients for these three polymorphs. In a later paper[8] they calculate the effect of hydrostatic pressure on the lattice parameters and again theory agrees with experiment.

TABLE 8
Lattice Energies of HMX Polymorphs

Form	Experimental[5]	Theoretical[5, 6]
β	-180.29* kJ/mole	-180.23 kJ/mole
α		-179.15
γ	-166.94†	-168.24

* Derived from $\Delta H_{sublimation}$ = 175.2 kJ/mole[30]
† Derived from $\Delta H_{sublimation}$ = 161.9 kJ/mole[31]

Small[26] expected to write a paper on the relationships among the polymorphs of HMX "and other forms," but apparently did not do so.

Solvate complexes: HMX is known to form solid, stoichiometric solvate complexes with nearly a hundred organic solvents.[32, 33] The crystal structure of the 1:1 complex of HMX with dimethylformamide (DMF) has been determined by Cobbledick and Small[34] and commented on by other workers.[35, 36] The HMX molecules have the conformation of the α-HMX molecules, including the crystallographic two-fold symmetry, with slightly different bond angles and bond lengths. The DMF molecules are disordered about two sites in the lattice.

TNT: (CAS Name and Registry Number: 1,3,5-trinitro-2-methylbenzene, *[118-96-7]*; other names: 2,4,6-trinitrotoluene; Tritol; Trotyl). $C_7H_5N_3O_6$.

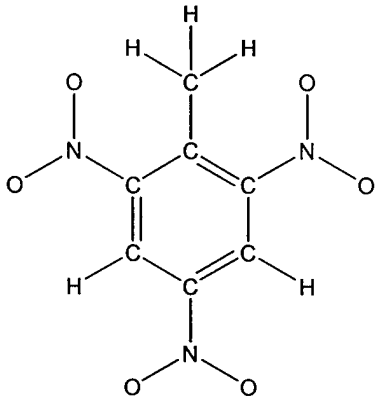

FIGURE 8. TNT

TNT exists in two principal crystalline forms. The monoclinic form is stable at room temperature through the melting point of 81°C. The orthorhombic form is metastable at room temperature, undergoes a solid-solid phase transition above 70°C, and then melts at 81°C. The monoclinic form normally shows extensive twinning.

The definitive X-ray determination of the structures of the two polymorphs is the work of J. R. C. Duke,[37] which is still classified a quarter-century later. However, the unit cell parameters he derived have been widely quoted in the literature (Table 9). Even the atomic coordinates in the unit cell of each polymorph, derived by Duke, are available; they have been deposited in the British Museum as supplementary document SUP 57198 by Gallagher, Roberts, Sherwood, and Smith.[38]

Golovina, Titkov, Raevskii, and Atovmyan[39] have also used X-ray diffraction to characterize TNT crystals. They use the first setting for describing the monoclinic crystal (with γ the angle between the *a* and *b* axes of the unit cell they choose) while Duke[37] and Gallagher *et al*[38] use the second setting (with β the angle between the *a* and *c* axes in the unit cell they choose). (See the Appendix for a discussion of the different conventions for describing monoclinic crystals.) Golovina *et al*[39] have also crystallized a variant of the orthorhombic form which has the longest cell length doubled (a = 40.0 Å. instead of 20.041 Å in the space group chosen, cf. Table 9).

TABLE 9
Crystal Structures of TNT

Form	Space Group	*a*	*b*	*c*	Angle	Z	Authors
Monoclinic	$P2_1/c$ (C_{5h}^5)	21.275	6.093	15.025	$\beta = 110.23°$	8	Duke, in Gallagher *et al*[38]
	$P2_1/b$ (C_{2h}^5)	21.407	15.019	6.0932	$\gamma = 111.00°$	8	Golovina *et al*[39]
Orthorhombic	$Pb2_1a$	15.005	20.024	6.107	-	8	Duke, in Gallagher et al[38]
	$P2_1ca$	20.041	15.013	6.0836	-	8	Golovina *et al*[39]
Orthorhombic		40.0	14.89	6.09			Golovina *et al*[39]

In each polymorph, there are two kinds of TNT molecules, four "A" molecules and four "B" molecules. While the two *ortho*-NO_2 (nitro-) groups adjacent to the -CH_3 group on the benzene ring are chemically equivalent in the isolated molecule or in solution, in each crystalline form they occupy geometrically different positions. So the A form and the B form of the molecule in each crystalline form each have three different kinds of nitro groups. The angle that the plane of each three-atom -NO_2 group makes with the plane of the hexagonal benzene ring is different for each of the three nitro-groups in each form of the molecule. Gallagher *et al*[38] and Golovina *et al*[39] provide complete descriptions of the bond lengths and bond angles. The twist angles of the nitro groups for the A molecules and B molecules in each polymorph are compared in Table 10. In each case, the smallest twist angle occurs for the -NO_2 group in the *para*-position on the ring (which has small hydrogen atoms on the neighboring carbon atoms). The *ortho*-nitro groups neighbor the more bulky -CH_3 (methyl) group; in each case, they twist by different amounts in the 40 - 60° range.

In each polymorph, the monoclinic and the orthorhombic, there are large differences between each twist angle in the A molecule and the corresponding twist angle in the B molecule. But the correspondence between each twist angle in the A molecule of the monoclinic form with the same twist angle in the A molecule in the orthorhombic form is astonishingly close; the same holds true for the B molecules in each crystalline form (Fig.9). Normally one sees much greater differences in the conformations of flexible groups or molecules between different polymorphs.

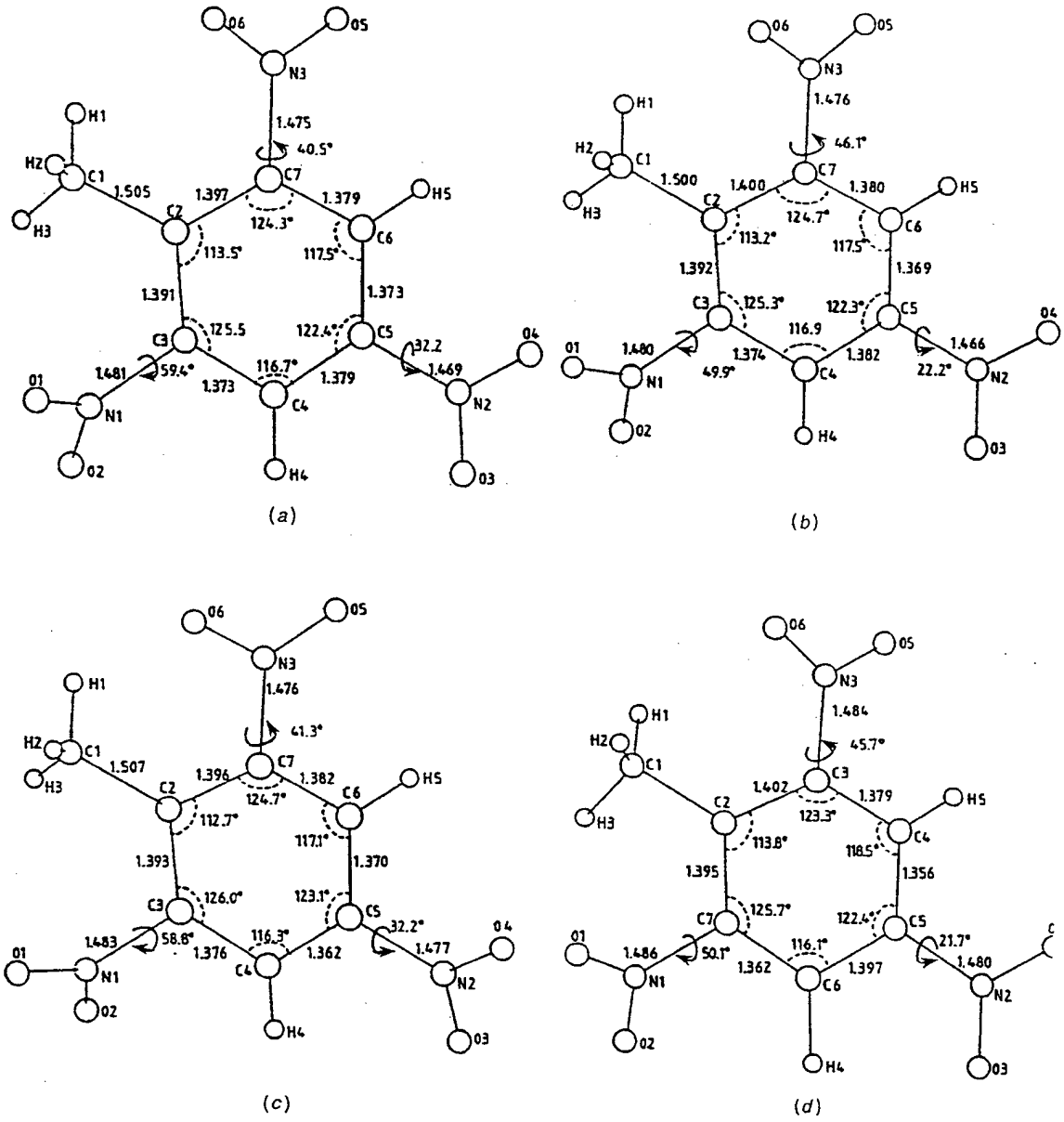

FIGURE 9. The bond lengths and bond angles of *(a)* the "A" molecule in monoclinic TNT; *(b)* the "B" molecule in monoclinic TNT; *(c)* the "A" molecule in orthorhombic TNT; and *(d)* the "B" molecule in orthorhombic TNT (from Gallagher, Roberts, Sherwood & Smith[38])

TABLE 10
Ring-NO_2 twist angles in TNT

	Monoclinic			Orthorhombic	
	Duke[37, 38]	Golovina[39]		Duke[37, 38]	Golovina[39]
A:	59.4°	60.3°	A:	58.8°	56.5°
	32.2°	33.0°		32.2°	33.4°
	40.5°	40.5°		41.3°	41.4°
B:	49.9°	50.5°	B:	50.1°	54.8°
	22.2°	22.5°		21.7°	22.5°
	46.1°	46.3°		45.7°	46.3°

Gallagher and Sherwood[40, 41] and Vrcelj, Gallagher, and Sherwood[42] have done extensive studies on growing TNT crystals of both polymorphs and on the twinning that occurs extensively in most preparations of the monoclinic phase. The similarity of the monoclinic and orthorhombic structures is shown in Fig. 10. The nature of the twinning in the monoclinic form is best described by a direct quote[41] and by a figure shown in their later paper[38] (Fig.11).

> Although the choice of solvent and crystallisation conditions must play an important role, the occurrence of twinning depends mainly on the internal structure of the crystal. In the monoclinic form, the almost identical nature of the two molecular conformations of TNT in the unit cell gives rise to a pseudo-glide plane perpendicular to (100) [shown as PG in Fig.10*a*] relating successive molecular layers. During crystallisation the presence of this pseudo-symmetry element can promote a deviation from the normal stacking sequence of the layers leading to the formation of the twinned structure shown in [Fig. 11]. Above and below the twin plane the molecular layers are arranged according to their normal monoclinic packing order, although the two halves of the crystal are now related by rotation of 180° about an axis normal to the (100) plane. Across the boundary, however, a true glide plane [shown as G in Fig.10*b*] replaces the pseudo-glide plane resulting in a new stacking sequence corresponding to the more symmetrical orthorhombic structure. The model clearly demonstrates that twinning in this material originates from a simple stacking fault, corresponding to a relatively minor conformational change in the molecules of the faulted layer with very little effect on the C-H···O hydrogen bonds across the twin boundary. Once twinning has occurred, additional molecular layers are added in the normal sequence until a second mistake in stacking returns the crystal to its original orientation. Random repetition of the stacking fault leads to the formation of a multiply twinned crystal ...

Golovina *et al*[39] actually observed the transformation, without disintegration, of an orthorhombic single crystal into a monoclinic single crystal with registration of the axes, which is strong evidence for the correctness of the model.

The orthorhombic structure then can be viewed basically as a regular stacking of monoclinic twinning faults zig-zagging vertically in the orientation shown above. The second orthorhombic form observed by Golovina *et al*,[39] with the doubled *a* axis, probably results from stacking faults in the normal orthorhombic form.

Gallagher *et al*[38, 42] have calculated the lattice energies of the various crystalline forms by summing the intermolecular interactions out to 30 Å. Sorescu, Rice, and Thompson[7] have also done molecular packing and molecular dynamics calculations on TNT, including lattice energy calculations (Table 11). The monoclinic form is calculated by both groups to be more stable than the orthorhombic form by 0.54 kcal/mole, which is close to the two experimental measurements of 0.22 kcal/mole[41] and 0.27 kcal/mole.[43] As one would expect from the model and the relationship between the monoclinic and orthorhombic phases, the lattice energy of the twinned monoclinic structure is calculated to be slightly less stable than the monoclinic structure. Sorescu *et al*[7] also calculate the thermal expansion coefficients for the monoclinic phase of TNT.

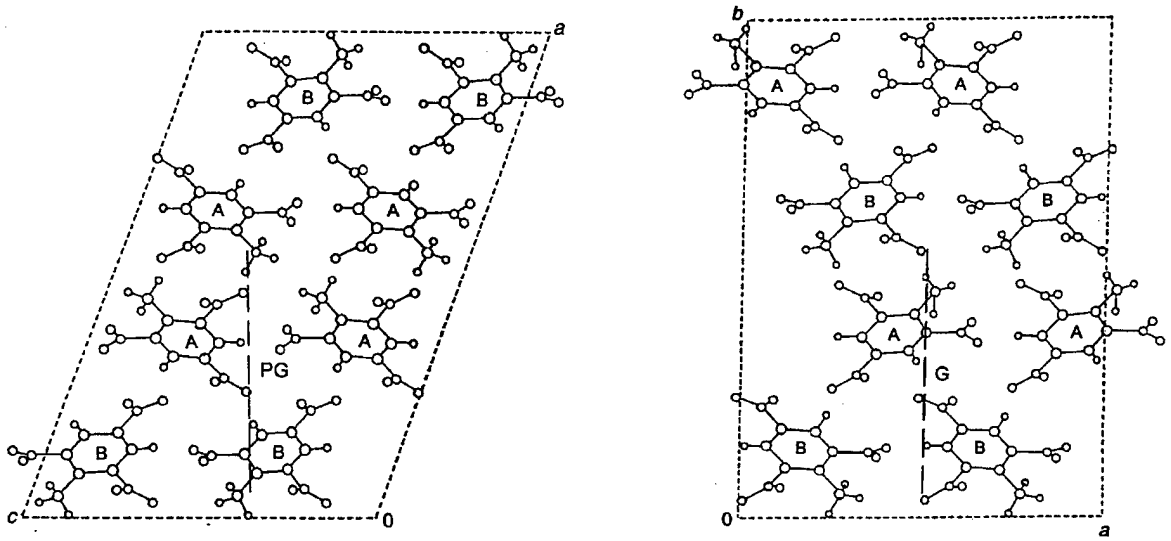

(a) *(b)*

FIGURE 10. *(a)* The projection of the 010 plane of the unit cell of monoclinic TNT, with PG showing the pseudo-glide plane. *(b)* The projection of the 001 plane of the unit cell of orthorhombic TNT, with G showing the glide plane. (from Gallagher, Roberts, Sherwood, and Smith[38])

Transforming the orthorhombic phase to the monoclinic phase requires cooperatively rotating the nitro groups on neighboring TNT molecules in layer after layer in the lattice[38,39]. The cooperative nature of such a phase transition would require a high activation energy despite the very small differences in the lattice energies of the two polymorphs. Golovina *et al*[39] have used X-rays to follow the orthorhombic to monoclinic phase transition as a function of time at several temperatures. They find an activation energy, E_a, of 85 kcal/mole. Such a high activation energy would account for the metastable nature of the orthorhombic phase at or near room temperature.

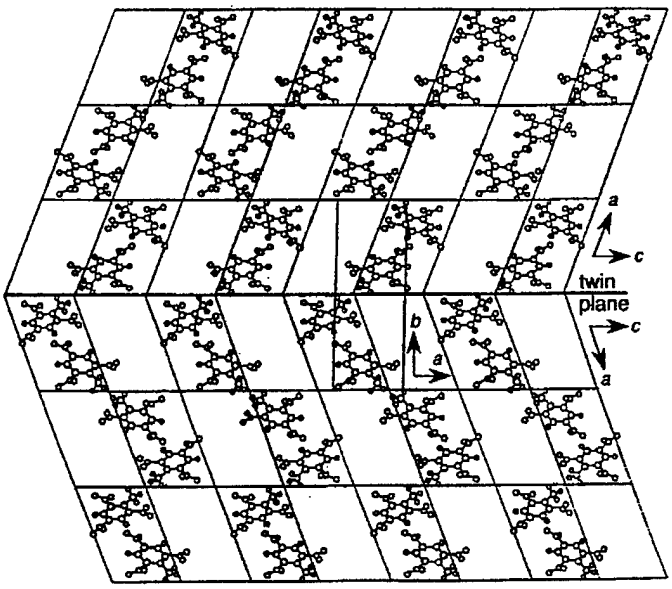

FIGURE 11. The twinning fault in monoclinic TNT with the orthorhombic stacking at the fault shown (Note: half the TNT molecules are not shown for clarity) (from Gallagher, Roberts, Sherwood, and Smith[38])

TABLE 11
Calculated lattice energies for TNT polymorphs

Form	Lattice Energy (Gallagher *et al*[38, 42])	Lattice Energy (Sorescu *et al*[7])
Monoclinic	-28.78* kcal/mole	-130.97 kJ/mole (= -31.30 kcal/mole)
Twinned monoclinic	-28.43 kcal/mole	
Orthorhombic	-28.24 kcal/mole	-128.70 kJ/mole (= -30.76 kcal/mole)

*The later paper[42] corrects an arithmetic error in the originally reported value[38] of -28.83 kcal/mole.

The older literature[12, 43, 44, 45, 46, 47, 48, 49] on the crystal structures and the crystal morphologies of TNT shows an early awareness on the part of many workers of the polymorphic nature of solid TNT, provides indications of the close structural relationship between the monoclinic and the orthorhombic forms (including common lines in the X-ray powder patterns), and provides evidence of doubled or tripled unit cell length varieties of both crystalline forms. Most of these observations are straightforwardly interpreted in terms of the crystal structures and models of Duke, Gallagher and Sherwood, and Golovina. Some of the older observations on longer repeat distances in some crystals require an extension of the twinning fault model of Gallagher and Sherwood.

A number of these older studies[43, 50, 51] also included heating curves with one or two peaks which are readily interpreted in terms of the X-ray studies of the orthorhombic to monoclinic phase transition by Golovina *et al*[39] and the differential scanning calorimetric (DSC) experiments on

monoclinic TNT and orthorhombic TNT by Gallagher and co-workers[41, 42]. In the latter work, monoclinic TNT shows only the melting point (at 355 K) while orthorhombic TNT shows a small peak at 345 K and a slightly suppressed melting point of 354 K.

Vrcelj, Gallagher, and Sherwood[42] concluded on the basis of their synchrotron radiation studies of the crystallization of purified TNT from various solvents and their DSC studies that the orthorhombic form always precipitates initially and that all but the poorest solvents (cyclohexanol, sometimes ethanol) mediate the conversion of the orthorhombic form to the monoclinic form.

Unfortunately, there do not appear to be published quantitative studies of the relative amounts of monoclinic TNT and orthorhombic TNT in explosive grade material. The best calorimetric data and the best X-ray data were obtained on highly purified, carefully crystallized materials. The one study[52] which used neutron diffraction to study bulk TNT in connection with the use of HNS to make better TNT casts didn't report any quantitative results on ordinary casts. (HNS is 2, 2′, 4, 4′, 6, 6′-hexanitro-stilbene.) This study found (as others have found) that quenching molten TNT can lead to the orthorhombic phase while slow cooling led to monoclinic TNT. They found that adding 0.5% HNS to the molten TNT produced a very uniform cast of very fine, randomly oriented grains of the monoclinic phase and that under no circumstances could they produce the orthorhombic phase. Neutron diffraction was used in this study because neutrons penetrate such samples better than X-rays and using the neutron beam at the NBS (now NIST) reactor, they could analyze an entire sample rather than a small region.

Because twinning can be so extensive in monoclinic TNT and because this twin fault is nearly identical in structure to the orthorhombic form, spectroscopic techniques will have difficulty in distinguishing, in explosive grade materials, between the extensively twinned crystalline regions of monoclinic TNT and an admixture of an equivalent amount of orthorhombic TNT with un-twinned monoclinic TNT. The distinctions which can be made between single crystal samples of these two polymorphs are difficult to make in polycrystalline cast samples of TNT.

Very rapid quenching of molten TNT (64°C/min.) can apparently lead to a glass, metastable below -15°C.[50] Upon heating, the glass transforms to the normal crystalline solid with an exotherm of 18.05 cal/gram between -14 and -8°C (ΔH_{fusion} = 23.53 cal/g for TNT).

Cady[15] found that TNT will crystallize from ethyl acetate solutions with conical faces with cone angles less than 180° and speculated that this may be connected to the polymorphism of TNT. (A fuller discussion of Cady's evidence and speculations is contained in the section below on PETN.)

PETN: (CAS Name and Registry Number: 2,2-bis[(nitrooxy)methyl]-1,3-propanediol dinitrate, *[78-11-5]*; other names: pentaerythritol tetranitrate). $C_5H_8N_4O_{12}$.

The highly symmetric PETN molecule has two common polymorphs.[53] PETN-I is stable up to 130°C (m.p. = 142.9°C) and crystallizes in a tetragonal lattice (a x a x c). PETN-II is stable from 130°C to its melting point (143.1°C) and crystallizes in an orthorhombic lattice (a x b x c). The unit cell parameters are given in Table 12. PETN-II rapidly transforms to PETN-I at temperatures below 130°C. Impurities in PETN-II can inhibit the transformation to the stable PETN-I.

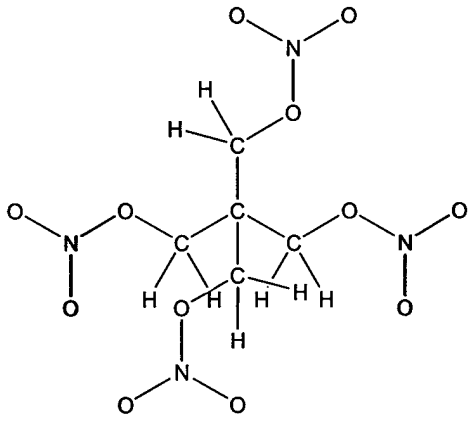

FIGURE 12. PETN

The detailed crystal structure of PETN-I was first worked out by Booth and Llewellyn[55], the structure was refined by Trotter[54] on the basis of the X-ray data of Booth and Llewellyn,[55] and further refined by Cady and Larson[53] on the basis of partial data on single crystal and on recrystallized samples. While Booth and Llewellyn found a shorter than normal carbon-carbon single bond and a much shorter than normal carbon-oxygen single bond, the later refinements of the structure lead to normal bond lengths and reasonable bond angles. The PETN molecule has four-fold alternating symmetry (an S_4 improper rotation axis) in PETN-I, giving each $-CH_2-O-NO_2$ group the same geometry around the central, close-to-tetrahedral carbon atom (two C-C-C angles of 109.2° and two of 109.9° instead of four at 109.5°). The two N-O bonds not involved in the bond to the carbon atom are not identical (that is, the $-NO_2$ group bonded to oxygen does not have two-fold symmetry).

TABLE 12
Crystal structures of PETN

Form	Space Group	*a*	*b*	*c*	Z	Density (meas.)	Density (calc.)	Authors
I	$P\bar{4}2_1c$ (D_{2d}^4)	9.38	-	6.70 Å	2	1.773	1.78	Booth & Llewellyn[55]
		9.380	-	6.709	2	1.778	1.778	Cady & Larson[53]
II	*Pcnb*	13.29	13.49	6.83	4		1.72 (136°C)	Cady & Larson[53]

Studies[53] of the PETN-II to PETN-I transition using a hot-stage microscope showed that there is a definite relationship between the crystallographic axes of the two polymorphs, and the X-ray diffraction pattern of PETN-II shows a close relationship to the rotation pattern of single crystal PETN-I.[53] The *c*-axis of PETN-II (6.83 Å) is almost the same length as that of PETN-I (6.709 Å), and the *a*- and *b*-axes in PETN-II, 13.29 and 13.49 Å, are close to the unit cell diagonal, $2^{1/2} \times a$ (= 9.38Å) = 13.27 Å, of PETN-I. The orthorhombic unit cell *a*- and *b*-axes of PETN-II, therefore, lie almost on the [110] and [1$\bar{1}$0] directions of the tetragonal unit cell of PETN-I (cf. Fig. A4(c) in the Appendix for a diagram showing the [110] and [1$\bar{1}$0] directions in the closely related cubic lattice.) Half of the PETN molecules in PETN-II have essentially the same geometry and orientation as half of the PETN

molecules in PETN-I. The other half of the PETN molecules in PETN-II are mirror image molecules, having had the $-CH_2-O-NO_2$ groups rotated a little less than 180° about the C-C single bond, the entire molecules rotated by nearly 60° about the *c*-axis, and the molecular centers translated about 1 Å in the *c* direction. While the space group for PETN-II does not require the four-fold alternating symmetry for the PETN molecules that the space group for PETN-I requires, there is apparently little distortion from this symmetry in PETN-II. The bond lengths and bond angles for all but the hydrogen atoms (which are poorly determined) are given in Table 13.

Cady and Larson[53] provide a clear, step-by-step explanation of how PETN-II can transform to PETN-I by a low activation energy route which involves neither cooperative motions of several molecules simultaneously nor steps involving strong intermolecular forces. The ready transformation of the high temperature form to PETN-I at temperatures below 130°C supports such a model. The calculations of Sorescu *et al*[7] on the lattice energies of the two polymorphs agree with the experimental results that PETN-I is more stable at room temperature than PETN-II.

TABLE 13
Bond lengths and bond angles in PETN-I and PETN-II (from Cady and Larson[53])

	PETN-I	PETN-II
r(C-C)	1.536 Å	1.537, 1.539 Å
r(C-O)	1.434	1.433, 1.433
r(O-N)	1.397	1.392, 1.386
r(N-O)	1.207, 1.222	1.212, 1.203;1.229, 1.222
∠ C-C-C	109.2, 109.9°	109.3, 109.4, 109.5, 109.8°
∠ C-C-O	107.5	107.5, 107.7
∠ C-O-N	115.9	117.4, 117.9
∠ (C)-O-N-O	113.3, 117.8	112.3, 119.2; 112.1, 120.3
∠ O-N-O	128.8	128.1, 127.5

Sorescu *et al*[7] use the intermolecular potential developed for nitramine crystals to calculate the lattice energies for the PETN polymorphs (Table 14).

TABLE 14
Lattice Energies for PETN

Form	Lattice Energy
I	-170.51 kJ/mole (= -40.75 kcal/mole)
II	-156.88 kJ/mole (= -37.50 kcal/mole)

The calculated temperature expansion coefficients for the lattice parameters of PETN-I, however, are only a third of the reported experimental values.[56,57] In their later paper on the effects of hydrostatic pressure on the lattice parameters of PETN-I, Sorescu *et al*[8] get acceptable agreement with the experimental values[58] only up to about 5 GPa and their calculations deviate more in the 5 - 10 GPa range. They attribute the limited success of their calculations on PETN-I to their

use of a rigid molecule approximation for the flexible-armed PETN molecule.

It should be noted that none of the X-ray data sets obtained in the studies mentioned above are of really high quality, and the traditional *R* factor obtained after multiple stages of refinement doesn't approach that of the most accurate X-ray structures.

Urbanski[59] points out that obtaining PETN in a crystalline shape which allows an easy flow to achieve a high bulk density is an important practical problem, and he briefly reviews the preparation of different shapes of PETN crystals, including the needle form which pours with difficulty.

The enthalpy of fusion of PETN-I does show a wide variation which is dependent on the mode of preparation. Rogers and Dinegar[60] categorize three kinds of crystalline PETN. The morphology of the crystals, the external shape of the crystals and the facets shown, depends on the preparation method. The first shape is the so-called "tetragonal habit," showing the characteristic apex angles and little evidence of strain. It is prepared by the slow addition of water to an acetone solution of PETN. Single crystals of the "tetragonal" habit were prepared by the slow cooling of a PETN-saturated acetone-water solution and by evaporation of an acetone solution of PETN. Two lots of the "tetragonal" habit PETN showed $\Delta H_{fusion} = 36.8 \pm 0.4$ and 36.5 ± 0.5 cal/gram, while single crystals in this habit had $\Delta H_{fusion} = 37.4 \pm 0.3$ cal/gram. Ball milling polycrystalline samples of the tetragonal habit to increase the surface area by more than a factor of five had no effect on ΔH_{fusion}. Cady and Larson[53] report $\Delta H_{fusion} = 38$ cal/gram for single crystals of PETN.

The second kind of PETN-I described by Rogers and Dinegar has a "needle" or "hour-glass" habit, with reentrant cavities on the ends of the needles and/or large length-to-width ratios. The needle habit is prepared by precipitating PETN from an acetone or acetone-methanol solution by the addition of water. They found about the same range of enthalpies of fusion for the needle habit as for the tetragonal habit, and grinding the needles to a fine powder ultrasonically had no effect on ΔH_{fusion}. Cady[15] shows a beautiful scanning electron microscope photo of what he terms "detonator grade" PETN which shows a rectangular parallelopiped crystal with a rectangular reentrant hole about 10 x 14 μ in a face about 16 x 20 μ at the end of a needle crystal.

The third kind of PETN-I described by Rogers and Dinegar is "superfine," consisting largely of irregular plates. It is prepared by rapidly pouring a relatively concentrated solution of PETN in acetone into cold water. They found ΔH_{fusion} varies from 31.7 ± 0.1 to 33.2 ± 0.2 cal/gram in various preparations. When they raised the temperature of the water used to precipitate the PETN, they found that ΔH_{fusion} rose until it reached 37.3 ± 1.0 cal/gram at a water temperature of 92°C. Cady and Larson[53] report $\Delta H_{fusion} = 32$ cal/gram for rapidly precipitated crystals.

Rogers and Dinegar showed that the magnitude of the surface area, the grinding of the crystals, and the presence of modest levels of impurities were not responsible for lowering the enthalpy of fusion. They attribute the decreased enthalpy of fusion to disorder of PETN molecules in the lattice, perhaps mixing molecules with orientations characteristic of PETN-II into PETN- I.

In a post-retirement talk on unsolved problems in the crystal structures of explosives, Cady[15] recounted his observation of a conical crystal face on the (110) face (cf. Appendix) of a large, transparent, apparently perfect PETN single crystal grown from an ethyl acetate solution. He found that various single crystals had cone angles of 179.8°, 179.6°, or 179.4°, and one had a cone angle of

178.5°. Each crystal face had only one such defect. The angle between the cone axes normal to (110) and the cone axes normal to (101) had the correct *a/c* ratio, but the actual face normals don't give the proper ratio. He found that the cone centers can be off in space and that the conical face can have both periodic and irregularly spaced spiral steps. He asks what the defect is, how it propagates with its center off in space and not in the crystal itself, what other defects are implied by such growth, and how the defect may be related to the formation of polytypic twins. (He found similar conical faces on TNT crystals and on RDX crystals grown from ethyl acetate solutions.)

Tetryl: (CAS Name and Registry Number: N-methyl-N,2,4,6-tetranitrobenzenamine, *[479-45-8]*; other names: N-methyl-N,2,4,6-tetranitroaniline; 2,4,6-trinitrophenylmethylnitramine; picrylmethylnitramine; N-2,4,6-tetranitro-N-methylaniline; Pyronite).

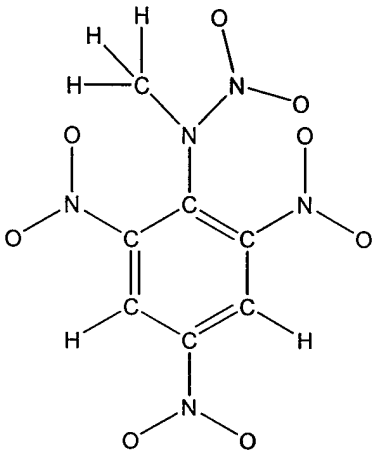

FIGURE 13. Tetryl

Tetryl (Fig. 13) has three $-NO_2$ (nitro) groups in alternating positions on the benzene ring, like TNT, but has an *N*-methyl nitramine group instead of the methyl group of TNT. Cady[61] has determined the monoclinic crystal structure (Table 15).

TABLE 15
Crystal structure of tetryl

Space Group	*a*	*b*	*c*	β	Z	Density (meas.)	Density (calc.)
$P2_1/c$ (C^5_{2h})	14.129	7.374	10.614 Å	95.07°	4	1.74	1.731

The four tetryl molecules in the unit cell have the same geometry (Fig. 14). As in TNT, the ring-nitro groups are twisted out of the plane of the benzene ring. The nitramine group is also twisted out of that plane. Each of the C-N bonds of the ring carbons is bent 3 - 5° out of the plane of the benzene ring, small enough to not make a significant contribution to the twist angles of the nitro groups (Table 16). In the solid, the $-CH_3$ group of the nitramine lies on the 6-side of the ring and the $-NO_2$ group of the nitramine lies on the 2-side of the ring.

TABLE 16
Twist angles in tetryl[61]

Group	Twist angle
2-nitro	25°
4-nitro	-23°
6-nitro	44°
Nitramine	65°

Analysis of the thermal motions of the NO_2-group in the nitramine shows that the NO_2-group is not free to oscillate about the N - N bond as a "free" NO_2 -group would. A weak intermolecular hydrogen bond between the C(5)-H of one molecule with the O(8) oxygen atom of the nitro-group in the nitramine of another appears strong enough to restrict the normal oscillation about the N - N bond and make the oscillatory motion occur about the N(5) - O(8) bond.

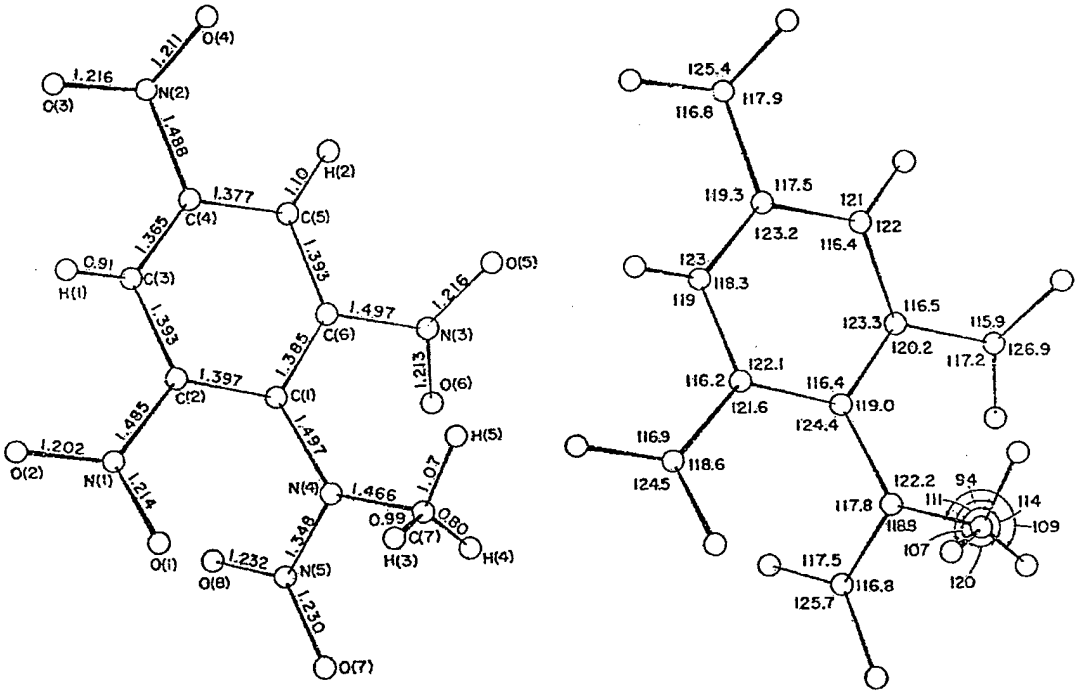

FIGURE 14. The bond lengths *(left)* and bond angles *(right)* in tetryl (from Cady[61])

Tetryl is known[62] to form a solid crystalline hydrate, $C_7H_5N_5O_8 \cdot 0.25\ H_2O$ when water is added to a solution of tetryl in acetone. The X-ray powder pattern shows that the unit cell of the hydrate has the same dimensions as that of tetryl itself, so the one water molecule per unit cell (four tetryl molecules) is presumably hydrogen bonded to oxygen atoms in nitro-groups. The authors of that study speculate that the oxygen atoms involved in hydrogen bonding to the water molecule are the oxygen atom of the nitramine nitro-group which is not involved in the intermolecular hydrogen bond with another tetryl molecule and an oxygen atom in a nitro-group in the 6-position of a different tetryl

molecule. The rationale is that there is a hole in the lattice that permits a water molecule to have O-H bond lengths (0.98 Å) and an H-O-H bond angle (104.66°), typical of water. This geometry corresponds to O-H···O distances of 2.51 Å, characteristic of strong hydrogen bonds.

The crystal lattice is disrupted upon heating between 113°C and 127°C as tetryl hydrate dehydrates, but the anhydrous tetryl recrystallizes, giving a sharp X-ray powder pattern, before melting. Urbanski[63] reports the melting point of pure tetryl to be 129.45°C. Urbanski also reports that for easy pouring of tetryl into molds, a mixture of coarse and fine tetryl crystals is preferred. Coarse crystalline tetryl is prepared by recrystallization from benzene, and fine crystalline tetryl is prepared by precipitation from acetone solution by the addition of water (just the method used to prepare tetryl hydrate). Unless the fine crystals are heated high enough and thoroughly dried, it is likely that such mixtures do contain tetryl hydrate as well as tetryl.

Acknowledgments

This work was supported in part by the FAA W. J. Hughes Technical Center, Atlantic City International Airport, New Jersey through Award DTFA0300X90011, the US Army (MIPR1BPIC00114), and the Office of Naval Research (ONR N0001401WX20564). GRM is a visiting faculty member under the ASEE/NRL summer faculty program.

Appendix

A brief review of some elements of crystallography

There are a quite a number of good treatments available of both the elements and the more advanced aspects of crystallography and most good libraries will have many of these.[64, 65, 66, 67, 68, 69] These references differ somewhat in their emphasis, mathematical approach, and level of sophistication. The purpose of this appendix is to provide a brief review of the most pertinent elements necessary to understand the crystal structures of the common explosives described in this review.

The focus in crystal structure studies is normally on a description of the size, shape, and symmetries of the fundamental repeating unit, the unit cell, and on the detailed geometry of the molecules and/or ions contained within the unit cell. There are seven conventional unit cells: cubic, tetragonal, orthorhombic, monoclinic, hexagonal, triclinic, and trigonal. The crystal structures encountered in this review do not involve the last two, so we will focus our attention on the first five.

The cubic unit cell (Fig. A1a) has the unit cell length along the x-axis equal to a. The unit cell length, b, along the y-axis is also equal to a, as is the unit cell length, c, along the z-axis. For a cubic unit cell, the x-, y-, and z-axes are at 90° to each other (the unit cell axes are orthogonal). The interaxial angles are denoted as α ($y \wedge z$), β ($z \wedge x$), and γ ($x \wedge y$). It is common, therefore, to describe the cubic unit cell as one in which $a = b = c$ and $\alpha = \beta = \gamma = 90°$.

The tetragonal unit cell (Fig. A1b) is also based on orthogonal unit cell axes, but only two of the unit cell lengths are the same. So $a = b \neq c$ and $\alpha = \beta = \gamma = 90°$. The orthorhombic unit cell (Fig. A1c) is also based on orthogonal unit cell axes, but the unit cell length along each axis is different. So $a \neq b \neq c$ and $\alpha = \beta = \gamma = 90°$.

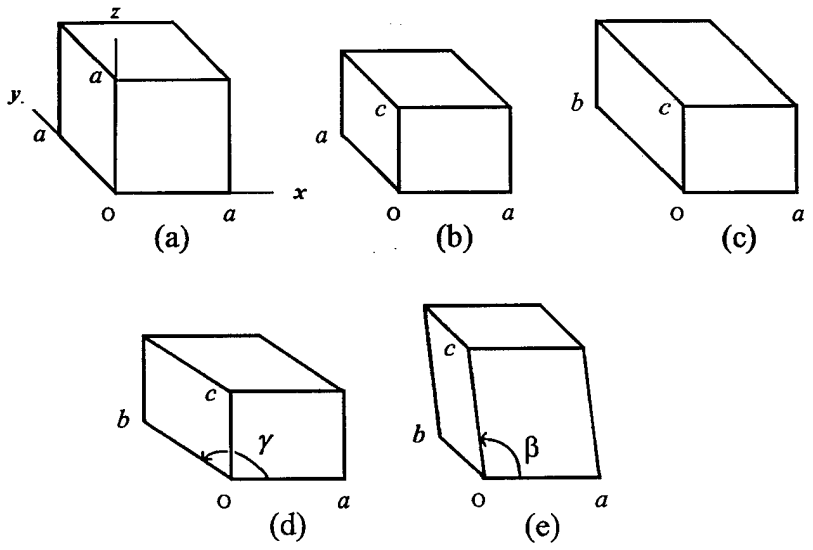

FIGURE A1. Unit cells. (a) Cubic; (b) Tetragonal; (c) Orthorhombic; (d) Monoclinic, setting 1 ($\alpha = \beta = 90° \neq \gamma$); (e) Monoclinic, setting 2 ($\alpha = \gamma = 90° \neq \beta$)

The monoclinic unit cell has unequal lengths along the *x*-, *y*-, and *z*-axes and one interaxial angle different from 90°. Crystallographers use one of two conventions, called "settings," to define the monoclinic unit cell. The first setting has $a \neq b \neq c$ and $\alpha = \beta = 90° \neq \gamma$ (Fig. A1d), and the second setting has $a \neq b \neq c$ and $\alpha = \gamma = 90° \neq \beta$ (Fig. A1e).

The unit cell for the hexagonal crystal system is not hexagonal in shape, but rather it is a prism with a diamond-shaped base. The diamond-shaped base, Fig. A2(a), is formed by two equilateral triangles sharing an edge, and has two 120° and two 60° interior angles. When three of these bases are arranged as shown in Fig. A2(b), a hexagon is formed in the *x*-*y* plane. Tilting the hexagon back to get a 3-D perspective of three unit cells yields Fig. A2(c), where $a = b \neq c$ and $\alpha = \beta = 90°$, $\gamma = 120°$.

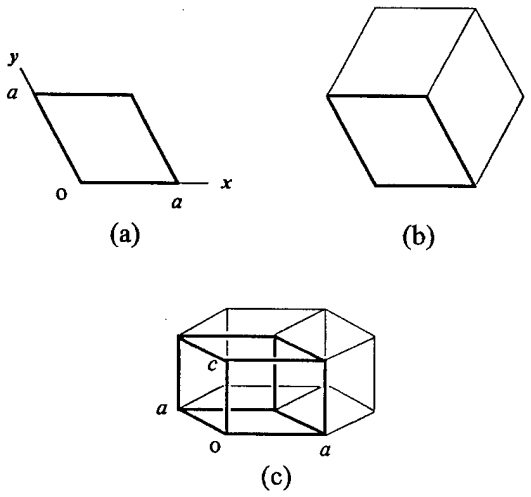

FIGURE A2. The hexagonal unit cell. (a) The base of the hexagonal unit cell in the *x*-*y* plane. (b) The bases of three unit cells sharing a point in the *x*-*y* plane. (c) Three unit cells forming a hexagon in the *x*-*y* plane.

The volume of the unit cell is *abc* for the unit cells with orthogonal axes, and *abc*(sin γ) or *abc*(sin β) for the first and second settings, respectively, of monoclinic crystals, and *abc*(sin γ) for hexagonal crystals. The number of formula units in the unit cell is abbreviated as *Z*; for crystals containing a single molecular compound, this is the number of molecules in the unit cell. It is conventional in crystal structure determinations to give the measured density of the crystal and the density calculated from the unit cell parameters and the molecular weight. In comparing different crystal structures for the same compound, it is often useful to compare the volume per molecule in the different polymorphs.

In addition to the two standard settings for monoclinic crystals, there are various other choices that crystallographers can make in defining unit cells. One can make different choices of which label (*a*, *b*, or *c*) to attach to the shortest unit cell length in an orthorhombic unit cell, for example, and which label to attach to the longest unit cell length. Different crystallographers may make different choices, and even the same crystallographers may, in some cases, choose the origin of the unit cell coordinates differently in different papers on the same crystal structure. While the *International*

Tables for Crystallography,[70] published by the International Union of Crystallography, contain the information necessary to relate different definitions of the same unit cell, the transformations between two different definitions aren't necessarily trivial.

The *International Tables* are organized by the space group, which describes the various kinds of symmetry which are present in the unit cell. Crystallographers prefer the Hermann-Mauguin symbols for the space groups while spectroscopists are usually more familiar with the Shoenflies symbols; both are given. In addition to giving information about the symmetry of each space group, the tables give the equivalent positions in the unit cell. The crystal structure paper normally will give the x-, y-, and z-coordinates for each atom in one molecule. If there are four identical molecules in the unit cell, one needs to generate the corresponding position of each atom in the other three molecules using these equivalent positions. A position is a set of x-, y-, and z-coordinates and, in this example, the tables will give the other three positions in terms of these three coordinates.

The symmetry elements characteristic of isolated molecules, such as a center of symmetry, mirror planes, and rotation axes, also exist in crystalline solids. One symmetry element that occurs only in crystalline solids and is useful for understanding the structures of some explosives is the "glide plane."

Two molecules are related by a glide plane when one can slide a molecule exactly half a unit cell length in the indicated direction and then, by reflecting the molecule in the glide plane, superimpose the first molecule on the second. The reflection makes the second molecule the mirror image of the first. Figure A3 shows a glide plane perpendicular to the page, the "sliding" is along the y-axis, and each object is turned into its mirror image. The lower-case p is translated up by $b/2$ and is reflected into its mirror image q , while the upper-case M is translated up by $b/2$ and reflected into its mirror image M, which is itself.

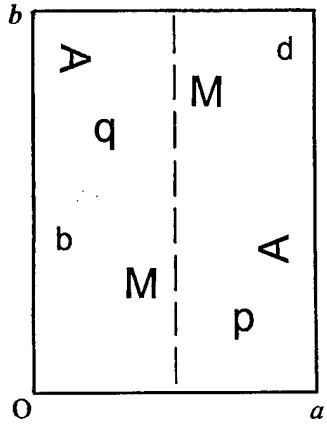

FIGURE A3. A glide plane (dashed line). An object is translated by $\pm b/2$ in the y-direction and reflected in the glide plane into the mirror image of the object. Here the upper-case letters are their own mirror image while the lower-case letters are not.

Frequently references are made to planes in the crystal or to directions in the unit cell. These are based on a system of Miller indices defining various planes in the crystal. The Miller indices h, k, and l for a particular plane, designated as the (hkl) plane, are the reciprocals of the intercepts that plane makes with the unit cell axes multiplied by the respective unit cell length. In Fig. A4a, the (111) plane in a cubic unit cell is shown. The plane intercepts the x-axis at a; the reciprocal of the unit cell intercept is $1/a$; h therefore is $(1/a)(a)$ or 1. Similarly $k = (1/a)(a) = 1$ and $l = (1/a)(a) = 1$. In Fig. A4b, the plane intercepts the x-axis at $a/2$, the y-axis at a, and there is no intercept (*i.e.*, it's at ∞) on the z-axis because the plane is parallel to the z-axis. So the Miller indices of this plane are calculated to be $h = (1/(a/2))(a) = 2$; $k = (1/a)(a) = 1$; and $l = (1/\infty)(a) = 0$, and the plane is designated as a (210) plane. In Fig. A4c, both the (110) plane and the (1$\bar{1}$0) (*one, bar-one, zero*) plane are shown. For the latter plane, the intercept on the y-axis is at $-a$, hence $k = (1/(-a))(a) = -1$; the minus sign is conventionally written as a "bar" over the "one," so the second Miller index is written as $\bar{1}$. Directions in the unit cell are usually given in terms of the normals to the planes, so the direction [111] is normal to the (111) plane, *etc.*

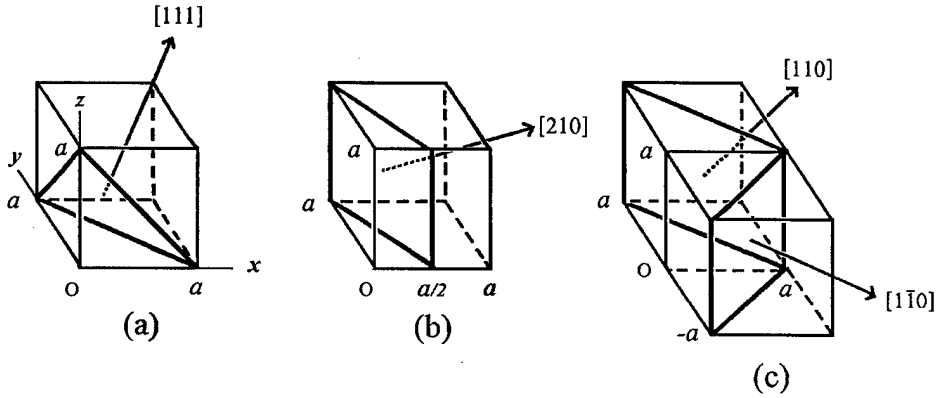

FIGURE A4. The Miller indices of planes (hkl) and the directions [hkl] normal to these planes in a cubic unit cell. (a) the (111) plane and the [111] direction; (b) the (210) plane and the [210] direction; (c) the (110) and the (1$\bar{1}$0) planes and the [110] and [1$\bar{1}$0] directions.

The external shape of crystals, the crystal morphology, though it must obviously be related to the internal structure of the crystal (the unit cell), can be influenced by the method of preparation and crystallization. Some solvents may promote faster growth along certain crystal axes and some impurities may do the same. The same unit cell may be found, for example, in needle-shaped crystals and plate-like crystals of a particular compound. These different shapes are referred to as different "habits."

References:

1. Mino R. Caira. *Crystalline Polymorphism of Organic Compounds*. Topics in Current Chemistry, **198**, 163-208 (1998).

2.Walter C. McCrone, *Polymorphism*, Chapter 8, pp. 725-767, in *Physics and Chemistry of the Organic Solid State,* Vol. II, Edited by David Fox, Mortimer M. Labes, and Arnold Weissberger. Interscience Publishers (John Wiley), New York. 1965.

3. D. C. Sorescu, B. M. Rice, and D. L. Thompson. J. Phys. Chem. **B, 101**, 798-808 (1997).

4. D. C. Sorescu, B. M. Rice, and D. L. Thompson. J. Phys. Chem. **B, 102**, 948-52 (1998).

5. D. C. Sorescu, B. M. Rice, and D. L. Thompson. J. Phys. Chem. **B, 102**, 6692-95 (1998).

6. D. C. Sorescu, B. M. Rice, and D. L. Thompson. J. Phys. Chem. **A, 102**, 8386-92 (1998).

7. D. C. Sorescu, B. M. Rice, and D. L. Thompson. J. Phys. Chem. **A, 103**, 989-98 (1999).

8. D. C. Sorescu, B. M. Rice, and D. L. Thompson. J. Phys. Chem. **B, 103**, 6783-90 (1999).

9. C. S. Choi and E. Prince, Acta Cryst. **B28**, 2857 (1972)

10. P.M. Harris and P.T. Reed. AFOSR-TR-59-165, 1959,. Ohio State University Research Foundation, Columbus, Ohio.

11. P. Terpstra, Z. Krist. **64**, 150-155 (1924)

12. R. Hultgren, J. Chem. Phys. **4**, 84 (1936)

13. T.P. Russell, P.J. Miller, G. J. Piermarini, and S. Block, Mat. Res. Soc. Symp. Proc. Vol. **296**, 199 (1993)

14. W. C. McCrone. Anal. Chem. **22**, 954 (1950)

15. H. H. Cady, Mat. Res. Soc. Symp. Proc. **296**, 243 (1993)

16. M. Pickering, J. Rylance, R. W. H. Small, and D. Stubley. Acta Cryst. **B47**, 782-789 (1991).

17. Tadeusz Urbanski, *The Chemistry and Technology of Explosives, Vol. 3*, Pergamon Press, 1967, p. 77ff. *Vol. IV*, 1984, p. 372ff..

18. W. C. McCrone, Anal. Chem. **22**, 1225-26 (1950)

19. Howard H. Cady and Louis C. Smith, *Studies on the Polymorphs of HMX*, Report No. LAMS-2652, Los Alamos Scientific Laboratory. Report distributed: May 3, 1962.

20. a. W. Selig. Explosivestoffe **17**, 73, 201 (1969)
b. H. Koenen, K.H. Ide, and K.H. Swart. Explosivstoffe **9**, 30 (1961)
c. H. H. Licht. 2nd Symposium on Stability of Explosives, p. 78, Tyringe, 1970
Work cited in, and Figure 57 shown in, Tadeusz Urbanski, *The Chemistry and Technology of Explosives, Vol. 4,* Pergamon Press, 1984. pp. 383-384 (1984)

21. Tadeusz Urbanski, *The Chemistry and Technology of Explosives, Vol. 4*, Pergamon Press, 1984. Table 6.3, p.383.

22. C. S. Choi and H. P. Boutin, Acta Cryst. **B26**, 1235-1240 (1970)

23. H. H. Cady, A. C. Larson, and D. T. Cromer, Acta Cryst. **16**, 617 (1963)

24. P. E. Eiland and R. Pepinsky, Z. Kristallogr. **106**, 273-298 (1955)

25. R. W. Armstrong, H. L. Ammon, Z. Y. Du, W. L. Elban, and X. J. Zhang. Mat. Res. Soc. Symp. Proc. **296**, 227-232 (1993).

26. P. Main, R. E. Cobbledick, and R. W. H. Small. Acta Cryst. **C41**, 1351-54 (1985).

27. M. Hermann, W. Engel, and N. Eisenreich. Z. Krist. **204**, 121-28 (1993).

28. R. E. Cobbledick and R. W. H. Small. Acta Cryst. **B30**, 1918-1922 (1974).

29. M. Juez-Lorenzo, V. Kolarik, M. Herrmann, W. Engel, and N. Eisenreich. Fresenius J. Anal. Chem. **349**, 163-65 (1994).

30. J. M. Rosen and C. Dickinson. J. Chem. Eng. Data **14**, 120 (1969)

31. J. W. Taylor and R. J. Crookes. J. Chem. Soc., Faraday Trans. 1, **72**,723 (1976).

32. R. S. George, H. H. Cady, R. N. Rogers, and R. K. Rohwer. Ind. Eng. Chem. Prod. Res. Develop. **4**, 209-214 (1965).

33. a. W. Selig. Propellants Explos. **7**, 70-77 (1982).
b. W. Selig. Explosivstoffe **17**, 73-86 (1969).
c. W. Selig. Explosivstoffe **15**, 76-87 (1967).

34. R. E. Cobbledick and R. W. H. Small. Acta Cryst. **B31**, 2905-08 (1975).

35. T. M. Haller, A. L. Rheingold and T. B. Brill. Acta Cryst. **C39**, 1559-63 (1983).

36. Richard E. Marsh. Acta Cryst. **C40**, 1632-33 (1984).

37. J. R. C. Duke. *Crystallography of TNT.* ERDE Report WAA 264/040 (1974).Classified. Crystallographic data reported in reference 38.

38. H. G. Gallagher, K. J. Roberts, J. N. Sherwood, and L. A. Smith. J. Mater. Chem., **7**(2), 229-235 (1997).

39. N. I. Golovina, A.N. Titkov, A. V. Raevskii, and L. O. Atovmyan. J. Solid State Chem. **113**, 229-238 (1994)

40. H. G. Gallagher and J. N. Sherwood. Mat. Res. Soc. Symps. Proc. **296**, 215-219 (1993).

41. H. G. Gallagher and J. N. Sherwood. J. Chem. Soc., Faraday Trans. **92**, 2107-16 (1996).

42. R. M. Vrcelj, H. G. Gallagher, and J. N. Sherwood. J. Am. Chem. Soc. **123**, 2291-95 (2001).

43. D. G. Grabar, F. C. Rauch, and A.J. Fanelli. J. Phys. Chem. **73**, 3514 (1969).

44. E. Hertel and G. H. Römer. Z. Physikal. Chem. **B11**, 77-89 (1930).

45. L. A. Burkardt and J.H. Bryden. Acta Cryst. **7**, 135 (1954).

46. W. R. Carper, L. P. Davis, and M. W. Extine. J. Phys. Chem. **86**, 459-62 (1982).

47. W. C. McCrone. Anal. Chem. **21**, 1583-4 (1949).

48. W. C. McCrone. Micro. Chem. J. Symp. Ser. **2**, 243 (1962).

49. M. C. Chick, W. Connick, and B. W. Thorpe. J. Cryst. Growth **7**, 317-26 (1970).

50. F. G. J. May, W. W. Thorpe, and W. Connick. J. Cryst. Growth **5**, 312 (1969).

51. W. Connick, F. G. J. May, and B. W. Thorpe. Aust. J. Chem. **22**, 2685-88 (1969).

52. S. F. Trevino, S. Portnoy, and C. S. Choi. *Effects of HNS on Cast TNT.* Memorandum Report ARLCD-MR-79001. 11 September 1979.

53. H. H. Cady and A. C. Larson. Acta Cryst. **B31**, 1864-1869 (1975).

54. J. Trotter. Acta Cryst. **16**, 698-99 (1963).

55. A. D. Booth and F. J. Llewellyn. J. Chem. Soc. **1947**, 837.

56. J. S. Chickos. In *Molecular Structure and Energetics*; J. F. Liebman and A. Greenberg, Eds; VCH Publishers Inc., New York, 1987, Vol. 2.

57. G. Edwards. Trans. Faraday Soc. **49**, 152 (1953).

58. B. Olinger, P.M. Halleck, and H. H. Cady. J. Chem. Phys. **62**, 4480-83 (1975).

59. Tadeusz Urbanski, *The Chemistry and Technology of Explosives, Vol. 4*, Pergamon Press, 1984, p. 310. *Vol. 2*, 1965, p. 177

60. R N. Rogers and R. H. Dinegar. Thermochim. Acta **3**, 367-78 (1971).

61. H. H. Cady. Acta Cryst. **23**, 601-09 (1967).

62. A. Gupta, M. Kaiser, G. Krien, and U. Ticmanis. Thermochim. Acta **167**, 49-56 (1990).

63. Tadeusz Urbanski, *The Chemistry and Technology of Explosives, Vol. 3*, Pergamon Press, 1967, pp.40-62.

64. Christopher Hammond. *Introduction to Crystallography, Revised Edition*. Microscopy Handbooks No. 19. Oxford University Press. Royal Microscopical Society. c1992

65. Walter Borchardt-Ott. *Crystallography, Second Edition*. Springer-Verlag. c1995

66. M. F. C. Ladd. *Symmetry in Molecules and Crystals*. Ellis Horwood Ltd. Halsted Press division of John Wiley & Sons. c1989

67. Joseph V. Smith. *Geometrical and Structural Crystallography*. John Wiley & Sons. c1982

68. R. Mirman. *Point Groups, Space Groups, Crystals, Molecules*. World Scientific. c1999

69. Simon L. Altmann. *Band Theory of Solids: An Introduction from the Point of View of Symmetry.* (Chapter 4). Clarendon Press, Oxford University Press. c1991

70. Theo Hahn, Editor. *International Tables for Crystallography. Volume A: Space-Group Symmetry. Fourth Revised Edition*. International Union of Crystallography. Kluwer Academic Publishers. c1995